

Miralha Lorraine (Orcid ID: 0000-0003-1448-9321)
Wissler Austin (Orcid ID: 0000-0001-8368-0053)
Bladon Kevin D. (Orcid ID: 0000-0002-4182-6883)

Characterizing stream temperature hysteresis in forested headwater streams

Running title: Stream temperature hysteresis

Lorraine Miralha¹, Austin D. Wissler¹, Catalina Segura¹, Kevin D. Bladon¹

¹ Department of Forest Engineering, Resources, and Management, Oregon State University,
Corvallis, OR, USA 97331

Corresponding Author: Lorraine Miralha, 3100 SW Jefferson Way, Corvallis, OR 97331, E-mail: lorraine.miralha@oregonstate.edu

This article has been accepted for publication and undergone full peer review but has not been through the copyediting, typesetting, pagination and proofreading process which may lead to differences between this version and the [Version of Record](#). Please cite this article as doi: [10.1002/hyp.14795](https://doi.org/10.1002/hyp.14795)

This article is protected by copyright. All rights reserved.

Accepted Article

Abstract

Stream temperature (T_s) is a key water quality parameter that controls several biological, ecological, and chemical processes in aquatic systems. In forested headwaters, exchanges of energy across air-water-streambed interfaces may influence T_s regimes, especially during storm events as the sources of runoff change over space and time. Analysis of the hysteretic behavior of T_s during storm events may provide insights into rainfall-runoff responses, but such relationships have not been thoroughly investigated. As such, our objectives were to (a) quantify the variability of stream temperature hysteresis across seasons in different sub-regions and (b) investigate the relationship between the hysteretic response and catchment characteristics. T_s hysteresis during storm events was assessed based on the hysteresis index (HI), which describes the directionality of hysteresis loops, and the temperature response index (TRI), which indicates whether T_s increased or decreased during a storm event. We analyzed T_s data from ten forested headwater reaches in two sub-regions (McGarvey and West Fork Tectah) in Northern California. We also performed a clustering analysis to examine the relationship among HI, TRI, topographic metrics, and meteorological characteristics of the study areas. Overall, the hysteretic behavior of T_s varied across seasons—the greatest HI occurred during spring and summer. Interestingly, in the McGarvey streams the variability in T_s hysteresis co-varied strongly with topographic metrics (i.e., upslope accumulative area, average channel slope, topographic wetness index). Comparatively, in West Fork Tectah the variability of T_s hysteresis co-varied most strongly with meteorological metrics (i.e., antecedent rainfall events, solar radiation, and air temperature). Variables such as the gradient between stream and air temperatures, slope, and wetted width were significant for both sub-regional hysteretic patterns. We posit that the drivers of T_s response during storms are likely dependent on catchment physiographic characteristics. Our study also

illustrated the potential utility of stream temperature as a tracer for improving the understanding of hydrologic connectivity and shifts in the dominant runoff contributions to streamflow during storm events.

KEYWORDS

Northern California, Redwood Forest, hydrologic response, k-means clustering, hydrologic connectivity, catchment physiography, rainfall-runoff processes

1. INTRODUCTION

Stream temperature (T_s) is a critical water quality parameter that influences dissolved oxygen solubility (Fellman et al., 2015; Loperfido et al., 2009; Ozaki et al., 2003), biochemical processes (Demars et al., 2011), aquatic habitat (Brewitt et al., 2017), and is important for sensitive aquatic species such as salmonids (Caissie, 2006; Hester and Doyle, 2011; MacDonald et al., 2014). In forested headwater catchments, the thermal regime in streams is the combined result of energy exchange across the air-water interface, between the stream bed and banks, and through advective transport via groundwater or hyporheic upwelling (Moore et al., 2005; Webb et al., 2008). Recent literature has elucidated the influence of groundwater inflow (Briggs et al., 2018; Larsen and Woelfle-Erskine, 2018; Snyder et al., 2015), hyporheic exchange (Briggs et al., 2012; Surfleet and Louen, 2018; Wondzell and Gooseff, 2013), and hillslope derived throughflow (Leach and Moore, 2017, 2015; Uchida et al., 2002) on stream temperature variability across a range of scales. However, research assessing T_s change during storm events in forested headwaters has been limited (Hebert et al., 2011).

Few have assessed the influence of storm events on the stream longitudinal thermal regime. For instance, during storm events, quickflow from shallow subsurface stormflow or preferential soil channels can strongly influence stream temperatures (Lange and Haensler, 2012; Leach and Moore, 2014; Subehi et al., 2010), despite precipitation heat flux often representing only 1–2% of the total heat flux reaching the stream (Hebert et al., 2011; Webb and Zhang, 1997). Others have linked seasonally variable antecedent moisture conditions (Lange and Haensler, 2012; Subehi et al., 2010), meteorological conditions (Herb et al., 2008; Somers et al., 2016), and catchment topography (Leach et al., 2017; Subehi et al., 2010) to T_s dynamics during storm events. The results from these previous studies suggest that the storm event responses in

stream temperature likely vary with both regional meteorological and catchment-scale topographic characteristics, such as local precipitation patterns (Croghan et al., 2019) or catchment slope (Subehi et al., 2010).

Runoff generation in steep forested headwater catchments is often controlled by physiographic characteristics, such as geology and topography (Gabrielli et al., 2012; Gomi et al., 2010; Hangen et al., 2001; Zimmer and McGlynn, 2017), and by temporal variability in water inputs that drive catchment storage (Amatya et al., 2016; Dralle et al., 2018; Sidle et al., 2000). During a storm event, precipitation may be partitioned into different flow paths that ultimately contribute to streamflow over a range of transit times depending on factors such as rainfall intensity (Detty and McGuire, 2010), soil infiltration capacity (Gomi et al., 2010), antecedent moisture conditions (Lange and Haensler, 2012; Radke et al., 2019), and catchment storage capacity (Heidbüchel et al., 2012; Zimmer and McGlynn, 2017, 2018). In most forested catchments, soil hydraulic conductivity is typically high enough that infiltration excess overland flow is rare (Keppeler and Brown, 1998), except on bedrock outcrops or areas with extremely shallow soils (Uchida et al., 2002). Therefore, subsurface flow pathways commonly dominate during storm events, but the exact partitioning of water inputs into shallow subsurface flow and deeper groundwater flow paths may vary depending on soil characteristics, topography, and storm characteristics (Detty and McGuire, 2010; Gomi et al., 2010; Rinderer et al., 2014; H J Van Meerveld et al., 2015).

As different flow paths activate during storm events, the relationship between discharge and water quality parameters can change (Hood et al., 2006; Inamdar et al., 2011; Lloyd et al., 2016a). Research on various chemical and physical water quality parameters has often illustrated a cyclical relationship with discharge, which is known as hysteresis (Williams, 1989; Vaughan et

al., 2017; Aguilera and Melack, 2018; Mistick and Johnson, 2020). Examination of hysteresis loops has increased in the past several decades as techniques and metrics to facilitate these relationships have been developed. Specifically, hysteresis metrics have recently been developed to (a) quantify the direction, slope, and size of hysteretic loops, and (b) compare hysteretic relationships between storms and catchments (Liu et al., 2021; Lloyd et al., 2016b, 2016a).

During storm events, stream temperature may exhibit hysteretic behavior depending on the antecedent stream temperatures, shifts in inputs of subsurface or groundwater with different temperatures (Blaen et al., 2013; Kobayashi et al., 1999), or inputs of precipitation with different temperatures (Kobayashi et al., 1999; Subehi et al., 2010). For instance, clockwise hysteresis may occur during storms when air temperatures are greater than stream temperatures (Fellman et al., 2014). This behavior may indicate thermal transfer from shallow quickflow sources that warm the stream water during the rising limb of the hydrograph. In addition, hysteresis loops with a positive slope may indicate flushing of heat from the catchment that causes T_s to rise towards the hydrograph peak, while loops with a negative slope may indicate dilution of heat from the catchment (i.e., from deep-sourced groundwater or direct channel precipitation) (Kobayashi et al., 1999). While providing important insights into site-specific drivers of stream temperature, analysis of stream temperature hysteresis may also provide a valuable research tool to infer source areas and runoff generation pathways during storm events, especially in forested headwater catchments.

Forested headwaters represent the landscape features with the strongest connection between terrestrial and aquatic elements (Freeman et al., 2007; Schlosser, 1991), and are generally more reactive to inputs of precipitation than downstream reaches (Wilby et al., 2015). Thus unsurprisingly, there is continued interest in understanding the responsiveness of headwater

channels to perturbations at the management-relevant reach scale. For instance, there have been recent calls for riparian forest management practices to consider the variable hydrological connectivity inherent to forested headwaters (Kuglerová et al., 2014; Laudon et al., 2016; Tiwari et al., 2016). Certain locations along headwater channels in boreal systems have been measured to provide disproportionate contributions of runoff to streamflow given local topography and soil conditions. These discrete riparian inflow points (DRIPS) (Ploum et al., 2018) can have a large influence on stream water chemistry and temperature (Erdozain et al., 2020; Lowry et al., 2007), and require additional study to determine their influence on T_s during storm events. Similarly, topographic metrics, such as upslope accumulated area (UAA), topographic wetness index (TWI), and flow weighted slope (FWS) theoretically describe the location of saturated soil and subsurface water flow paths (Beven and Kirkby, 1979; Jencso et al., 2009). Variability in these metrics often explains areas of strong lateral groundwater influence in boreal regions (Leach et al., 2017) and elucidates topographic control on stream temperature in southern Alaska (Callahan et al., 2015). However, such an analysis has not been undertaken in steep, temperate conifer forests like the coast redwood (*Sequoia sempervirens*) dominated North Coast range of California, USA. Assessing the validity of these metrics for spatially and temporally identifying areas of a catchment that dominate runoff contributions, and influence stream temperature, can have important implications for quantifying available habitat and refugia to aquatic ecosystems. Moreover, improving understanding of the relationships between terrain wetness indices and stream temperature in various regions could enable assessments of catchment resilience or vulnerability to natural or anthropogenic disturbances.

As such, the objectives of our study were to investigate the response of forested headwater streams to storm events by analyzing data collected from an array of distributed

Accepted Article

temperature sensors across ten catchments in Northern California. We were particularly interested in understanding (a) if stream temperature (T_s) hysteresis varied across seasons in forested headwater streams in different sub-regions and (b) whether there were differences in the relationships between stream thermal regimes and topographic and climatic variables across sub-regions. We first used metrics to quantify the magnitude and direction of hysteresis in the streamflow-stream temperature relationship during storm events to infer whether the relationships changed seasonally. Then, we performed a clustering analysis using meteorological characteristics and topographic metrics of hydrological connectivity to compare the hysteretic response to 23 storm events across ten headwater catchments. Our results revealed that T_s hysteresis varied across seasons in McGarvey and Tectah. Interestingly, while the T_s hysteresis observed in Tectah streams was most related to the meteorological metrics considered in this study, the hysteretic response in McGarvey streams was strongly connected to the topographic characteristics of the catchment. Overall, our study provided an investigation of T_s hysteretic behavior, storm characteristics, climate, and topography across headwater catchments. Our results also illustrated the need for additional research to improve our understanding of regional differences in the controls on thermal regimes in forested headwater streams, to facilitate site-specific forest and water policy and management decisions.

2. METHODS

2.1. Study locations

We collected data along ten headwater streams that drain into the Klamath River in the Northern California Coast Range, USA (Figure 1). The catchments ranged in area from 21 to 63 ha and were located in two distinct elevation ranges (Table 1). Five study streams (1 to 5) were

located along the West Fork Tectah Creek between 425–500 m elevation. The other group of five streams (11, 13, 14, 15, 18) were located along McGarvey Creek at elevations below 190 m. The two groups of study catchments were separated by approximately 25 km. Stream valleys are V-shaped with considerable channel incision and steep slopes (19–31°) (Woodward, Lamphear, & House, 2011). The streams also have narrow riparian areas, resulting in strong confinement and coupling between streams and hillslopes. All ten streams are characterized as perennial, step-pool systems (Fritz et al., 2020; Montgomery & Buffington, 1997) with a few small cascades. The average active widths of the study streams were all less than two meters, with average stream channel slopes ranging from 8–15 ° (Table 1). Surprisingly, while the streams are generally considered perennial, exceedingly dry weather during our study led to some stream sections going dry for short periods of time. Specifically, the mid-reach in streams 1, 3, and 14, and the most upstream portion of streams 11 and 13 went dry during the late summer months in July and August.

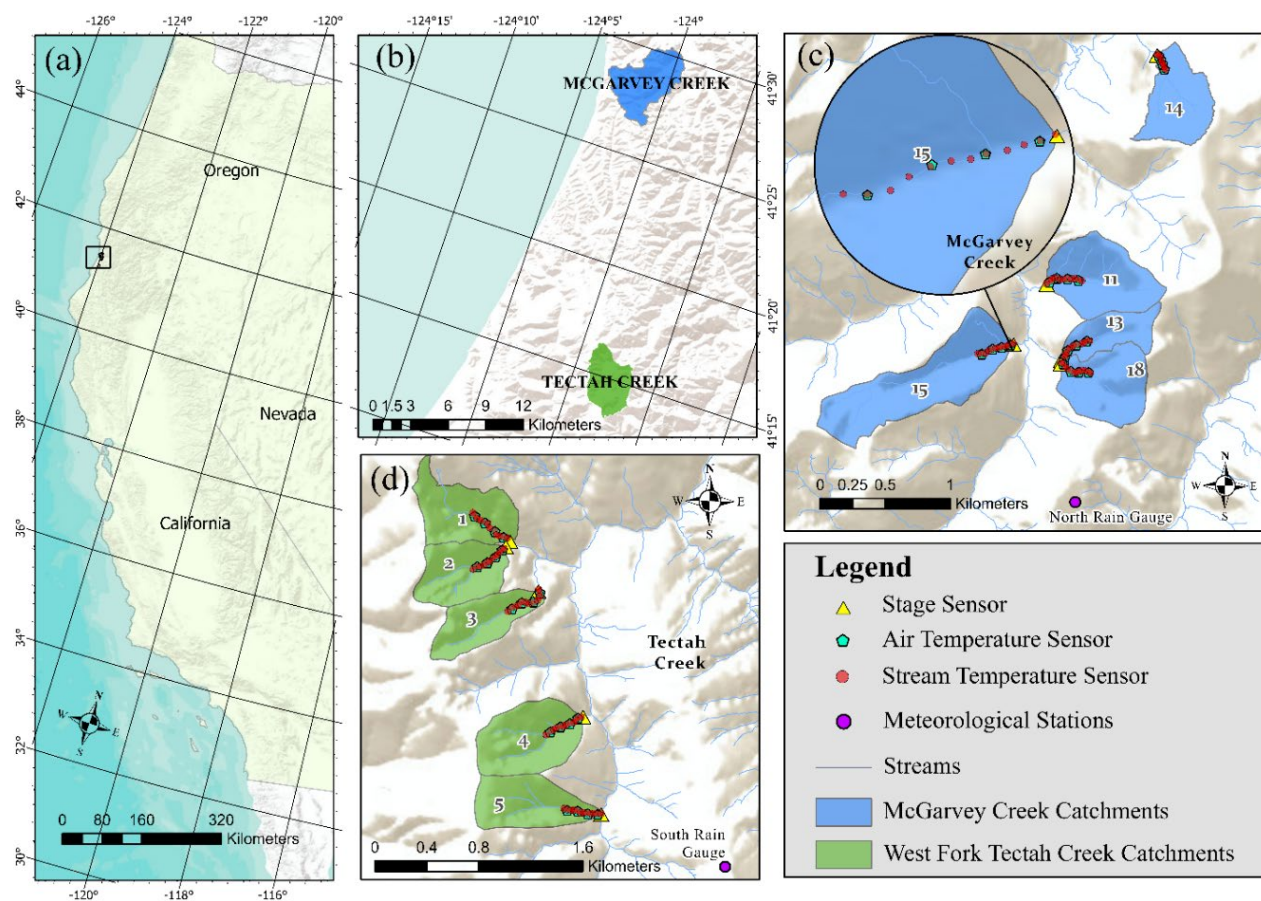


FIGURE 1 Maps of study area locations, including (a) general study location in Northern California, USA, (b) relative locations of McGarvey and Tectah Creeks, (c) study catchments in McGarvey Creek with zoomed view of the sensors, and (d) study catchments in West Fork Tectah Creek.

TABLE 1 Catchment and stream physical characteristics in each of the two sub-regions.

Sub-Region	Catchment Number	Catchment area (ha)	Average catchment elevation (m)	Monitored stream length (m)	T_s sensor spacing (m)	Average catchment slope (°) ^a	Average stream slope (°) ^a	Riparian canopy closure (%) ^b	Average active width (m)
Tectah	1	38	462	305	28	25	12	97.4	1.7
	2	30	450	305	28	25	8	92.4	1.9
	3	28	452	305	28	24	9	93.6	2
	4	37	450	305	28	24	11	96.4	1.8
	5	30	463	305	28	19	10	98.1	1.4
McGarvey	11	40	114	305	28	31	12	97.6	1.7
	13	21	153	305	28	25	15	97.2	1.9
	14	30	82	202	18	30	11	94.2	2
	15	63	85	305	28	27	12	99.6	1.8
	18	32	133	305	28	26	9	97	1.4

^a Derived from 1-meter DEM in ArcMap 10.8.1

^b The average value of six hemispherical photos spaced evenly along the riparian area adjacent to each monitored stream. Photos were analyzed using Hemi-View software (Delta-T Devices, Ltd., Cambridge, UK).

The climate in the study region is characterized as temperate and maritime with a distinct wet-dry seasonality and considerable influence from coastal fog (Dawson, 1998). Summers are warm and dry and winters are mild and wet, with average annual air temperatures between 11 and 12 °C (PRISM Climate Group, 2014). The majority of precipitation occurs as rainfall between October and May, with an average annual rainfall of 2,900 mm in Tectah Creek and 2,000 mm in McGarvey Creek (PRISM Climate Group, 2014). During the study period (October 1, 2019–June 15, 2020), local meteorological stations (Figure 1) recorded a total precipitation amount of 1,680 mm in McGarvey and 1,710 mm in Tectah. Accordingly, streamflow reaches an annual peak during mid-winter and an annual low during late summer.

Vegetation consists primarily of 30–60-year-old second-growth Douglas-fir (*Pseudotsuga menziesii*) and coast redwood (*Sequoia sempervirens*), with western red cedar (*Thuja plicata*) and western hemlock (*Tsuga heterophylla*) occurring at lower densities. Red alder (*Alnus rubra*) and tanoak (*Notholithocarpus densiflorus*) are common in riparian areas. Riparian canopy closure along the streams is very high (above 90%) and similar across streams

(Table 1). Soils are well-drained gravelly clay loams of the Coppercreek and Sasquatch series, with depths typically between 70 and 100 cm (Soil Survey Staff, NRCS, 2016). Field observations indicated increasing soil clay content with soil depth, with the uppermost soil layers composed of extremely well drained organic detritus. The lithology consists of marine-derived sedimentary and metasedimentary rock of the Franciscan Complex (Woodward et al., 2011).

2.2. Data collection

To quantify stream and air temperature, we installed 16 thermistors (Onset HOBO TidbiT v2, Bourne, MA; accuracy ± 0.21 °C) longitudinally along each study stream. This included 12 in-stream sensors, which were spaced approximately every 28 meters (except in stream 14 due to local site selection constraints, Table 1) along each stream (Figure 1) and four evenly spaced air temperature sensors, which were installed along the riparian corridor and approximately ~1 m above the stream. Data was collected at 15-minute resolution. Information about how the thermistors were installed and time series plots can be found in the supplementary material.

We measured stream stage at the downstream end of each stream with a pressure transducer (Levellogger Edge, Model 3001, accuracy: $\pm 0.05\%$, Solinst Canada Ltd., Georgetown, ON, Canada) housed in a PVC stilling well. A barometer (Barologger Edge, Model 3001, accuracy: ± 0.05 kPa, Solinst Canada Ltd., Georgetown, ON, Canada) was placed at the outlet of streams 1 and 11 to quantify atmospheric pressure for compensation of stream stage. Manual measurements of stream stage were taken with a ruler at the base of each stilling well to the nearest half centimeter during five field visits (approximately every two months) to derive continuous stage data from the pressure transducers.

We also installed two meteorological stations (Onset HOBO U30 Data Logger, Bourne, MA) during summer 2019. The stations were centrally located in each of the two study sub-regions, within ~3 km of all study streams (Figure 1). All data was collected at a 15-minute resolution. Information about the meteorological station data and plots of the data from these stations can be found in the supplementary material.

2.3. Data Analysis

We focused our analysis of T_s change during storm events that occurred during the wet season of the 2020 water year (October 1, 2019–June 15, 2020), but also included the first significant summer storms, which occurred in September 2019. Individual storm events were identified by ensuring there was at least 6 hours of no precipitation between two events (Driscoll et al., 1989). Initial analysis was limited to storm events with a minimum magnitude of 10 mm, as this depth of rainfall was visually determined as the threshold of rainfall necessary to achieve an in-stream response (i.e., a change in stream stage). This yielded 40 storm events for the Tectah Creek study area and 38 events for the McGarvey Creek study area. Refer to the supplementary material for more information about the storm analysis data preparation.

Hydrograph recession was assumed to end when stream stage reached the stage value closest to what it was at the beginning of a rainfall event by considering a period up to twice the storm duration following the end of each storm event. Therefore, storm duration was defined as the time from the onset of the first tip in the precipitation data to the time of hydrograph recession. Any storm event where stream stage did not recede to less than half the maximum stage before the onset of the next storm was excluded to constrain our analysis to storms with hydrographs that were not influenced by subsequent events. This resulted in 13 to 32 storms in McGarvey streams, and 17 to 27 storms in Tectah streams being carried forward for initial

analysis. Table S1 illustrates the storm events included and excluded per stream. Plots of the hydrographs of the storm events considered per stream can be found in the supplementary material (Fig. S1-S10). Due to equipment failure, stage data in stream 13 was only available for storms prior to January 24, 2020.

2.3.1. Storm hysteresis behavior

We also used hysteresis analysis to quantify the event-based temporal relationship between T_s and stream stage. We used the analysis to quantitatively assess how T_s in headwater catchments responded to precipitation inputs and changes in streamflow across seasons (Subehi et al., 2010). Hysteresis loops can be used to describe the shape, magnitude, direction, and slope of the stream temperature-stage relationship during storm events, where the slope of the loop and rotational direction (clockwise or counterclockwise) may be used to infer different flow pathways that contribute runoff during events (Aguilera and Melack, 2018; Evans and Davies, 1998). Because we had more than 1,700 plots of hysteresis loops (e.g., Figure S19 and S20), we used the hysteresis index (HI) (Lloyd et al., 2016b) to assess variable T_s responses to precipitation events among streams and through seasons. This HI is attractive for hysteresis analysis because it is dimensionless and constrained between 1 and -1, with positive values indicating clockwise hysteresis and negative values denoting counterclockwise hysteresis. Clockwise (Counterclockwise) direction indicated that T_s were warmer (cooler) on the rising limb than the falling limb of the storm hydrograph. The magnitude of the HI corresponded to the ‘fatness’ of the loop, where hysteresis loops with HI values close to $|1|$ had a greater area than those with HI values close to $|0|$. This index requires normalizing flow (stage) (Equation 1) and

temperature (Equation 2) values by the observed ranges for each storm to make comparisons possible among storms and catchments.

$$\text{Normalized } H_i(\text{stage}) = \frac{H_i - H_{\min}}{H_{\max} - H_{\min}} \quad (1)$$

$$\text{Normalized } T_i = \frac{T_i - T_{\min}}{T_{\max} - T_{\min}} \quad (2)$$

where H_i is the stream stage at time i , H_{\min} and H_{\max} are the minimum and maximum stage measured over the storm event, T_i is the stream temperature measured at time i , and T_{\min} and T_{\max} are the minimum and maximum stream temperature measured over the storm event.

The HI (Equation 3) was computed by finding the difference between temperature values on the rising and falling limb of the hydrograph for even intervals of the change in stage. This involved splitting the time series of stage and T_s for each storm into two sections — one prior to the peak stage and one after the peak stage value. We used 2 % intervals of normalized stage to compute differences in T_s on the rising and falling limb for each storm (Vaughan et al., 2017).

The average of these differences for each storm event is the HI.

$$HI = \frac{\sum(T_{RL_normalized} - T_{FL_normalized})}{n} \quad (3)$$

where $T_{RL_normalized}$ is the normalized temperature value at an interval of normalized stage on the rising limb of the hydrograph, $T_{FL_normalized}$ is the normalized temperature value at the same interval of normalized stage on the falling limb, and n is the number of rising limb-falling limb pairs. We calculated an HI value for every stream temperature monitoring location along each stream if the sensor was submerged at the start of the storm event.

We also calculated the temperature response index (TRI) to quantify whether T_s increased or decreased during the rising limb of the storm hydrograph (i.e., an index similar to the flushing index concept in the literature; Butturini et al., 2008; Vaughan et al., 2017) (Equation 4):

$$TRI = T_{peak_normalized} - T_{init_normalized} \quad (4)$$

where $T_{peak_normalized}$ is the normalized temperature value at the hydrograph peak, and $T_{init_normalized}$ is the normalized temperature value at the onset of precipitation. Similar to the HI, TRI is also constrained between -1 and 1. A positive TRI indicates stream temperatures increased on the rising limb of the event and heat was delivered, or flushed, to the stream. When TRI is negative, stream temperatures decreased during the rising limb, indicating heat was dissipated, or diluted, from the stream. A TRI value of 1 indicated that peak stream temperatures coincided with the peak stage value during an event. We removed storm events from our analysis if there were less than six of the ten catchments where we were able to compute HI or TRI values. This generally occurred when storm events weren't evident in the data from all catchments. This was done to prevent bias towards certain catchments where the data were more reliable. This enabled us to analyze 23 paired storm events across six or more of the ten catchments (Table S2).

2.3.2. Topographic analysis

We calculated several topographic metrics for each stream temperature monitoring location, including upslope accumulated area (UAA), topographic wetness index (TWI), and flow weighted slope (FWS). This was done to assess whether the magnitude and direction of hysteresis metrics describing the stream temperature response to storm events could be explained by indices that relate surface topography to runoff generation processes (Callahan et al., 2015; Leach et al., 2017). A primary assumption of all three metrics is that subsurface hydrologic flow pathways reflect surface topography. This may not be a valid assumption in areas with lithology characterized by extensive bedrock fractures, complex soil structure, or where bedrock and

surface topography are dissimilar (Genereux et al., 1993; Freer et al., 2002; Gabrielli et al., 2012; Segura et al., 2019), but requires further investigation.

Calculations were carried out using 0.25-meter resolution digital elevation models (DEMs) for both study areas in ArcMap 10.8.1. The DEMs were first preprocessed by coarsening to 1-meter resolution to remove minor topographic discrepancies and by filling sinks (Wang and Liu, 2006). To provide an upper and lower bound on the potential true value of each topographic metric at each sensor location, we calculated average, standard deviation, maximum and minimum values of UAA, TWI, and FWS for all cell locations on the stream channel within a three-meter radius of each snapped sensor location. Values of all three topographic metrics (UAA, TWI, and FWS) from within this three-meter radius were used to compute average point values, which were then used as predictors in our clustering analysis. More information about UAA, TWI, and FWI calculation and DEM processing can be found in the supplementary material.

2.3.3. Statistical Analysis

To evaluate the differences in hysteretic behavior across seasons, we first used quantile-quantile plots to check for normality of the data distributions and ran a Bartlett's test of variance homogeneity (Snedecor, 1956). The data failed to meet normality and equal variance assumptions, so we applied the non-parametric Kruskal-Wallis test, which was used to evaluate whether samples were from the same distribution. We chose the Kruskal-Wallis test because it is a robust non-parametric test (i.e., it does not rely on a specific data distribution), has higher statistical power when applied to distributions of unequal variance, and accommodates comparison among groups with unequal sample sizes (Mahoney and Magel, 1996; Siegel, 1957). To avoid Type-I error (i.e., falsely claiming a difference in hysteretic indices between seasons),

we ran a post-hoc Kruskal-Wallis multiple comparison test by Dunn (1964) using Benjamini-Hochberg method for multiple hypothesis testing at a 5% cut-off.

We applied a *k*-means clustering algorithm to evaluate the association between storm (i.e., meteorological) characteristics and topographic metrics with HI and TRI indices. *K*-means clustering is a partitioning unsupervised classification approach that aims to assemble observations with similar attributes into groups or clusters (Hartigan and Wong, 1979). This technique has been widely applied in hydrological studies for the identification of flow regimes (Olden et al., 2012), regional hydrological patterns (Aytaç, 2020; Sharghi et al., 2018; Tongal and Sivakumar, 2017), and flood-forecasting (Wu et al., 2015). To perform the analysis, we selected 51 environmental variables that described storm (meteorological), hydrologic, and topographic characteristics (Table S3). We ran the *k*-means algorithm three times. First, we performed an overall test (i.e., all the data) to detect the number of clusters formed regardless of catchment type. Then, we separated the dataset to perform an individual catchment clustering test (i.e., one for McGarvey and another for Tectah). We compared the between and within sum of squares (BSS/TSS) ratio and the total within-cluster sum of squares per test to evaluate the power of our results. Generally, clustering results are considered strong when the BSS/TSS ratio is close to one and the total within-cluster sum of squares is small (Kaufman and Rousseeuw, 2009).

To determine the optimal number of clusters (*k*), we applied the average silhouette method, which computes the average silhouette of observations for different values of *k*. The silhouette value measures how similar an observation is to its own cluster compared to other clusters (Rousseeuw, 1987). We used the optimal *k* that maximized the average silhouette over a range of possible *k* values (Kaufman and Rousseeuw, 1990). We also assessed the stability of the

Accepted Article

detected k value by running a cluster stability analysis based on the Jaccard similarity bootstrapping coefficient (J) (Hennig, 2007). This test sampled from the sample population n times to quantify how many times k was likely to dissolve or recover. Generally, a valid and stable cluster should yield a mean J value greater than or equal to 0.75 (Hennig, 2007 and more in the supplementary material). We compared the distribution of all variables in each cluster and used the Kruskal-Wallis test with post-hoc Dunn's tests to assess whether the distributions of HI and TRI differed per cluster. We performed this test for all meteorological, hydrologic, and topographic variables to enable a multi-comparison of the variability in distributions among clusters for both the HI and TRI values. Because we included data from all monitoring sensors and they were spaced every ~ 28 per site, we acknowledge our observations may not be truly considered independent.

3. RESULTS

3.1. Seasonal Storm Hysteresis

Hysteresis analysis yielded up to 12 hysteresis index (HI) and temperature response index (TRI) values per stream for each storm, corresponding to each measurement location of stream temperature. Interestingly, HI values varied in direction and magnitude between seasons, storm events, and catchments (Figure 2a). Positive HI values, indicating clockwise hysteresis, generally occurred during spring and summer events. Negative HI values, counterclockwise hysteresis, mainly occurred during fall and winter events (Figure 2b).

Despite the variability in HI values, we observed a general median seasonal trend in hysteretic behavior of stream temperature. HI values varied substantially from stream to stream, especially among the 10 streams during fall storms (Figure 2b; SD: 0.36). (). For example,

during fall storm events, the difference between the largest and smallest HI values from individual streams was 0.31 in Tectah and 0.55 in McGarvey (Table 2). In other words, during the fall storms we observed streams with no evidence of hysteretic behavior in stream temperature but observed strong hysteretic behavior in neighboring streams. For the remaining seasons, stream-average HI values were either all positive (summer) or all negative (winter).

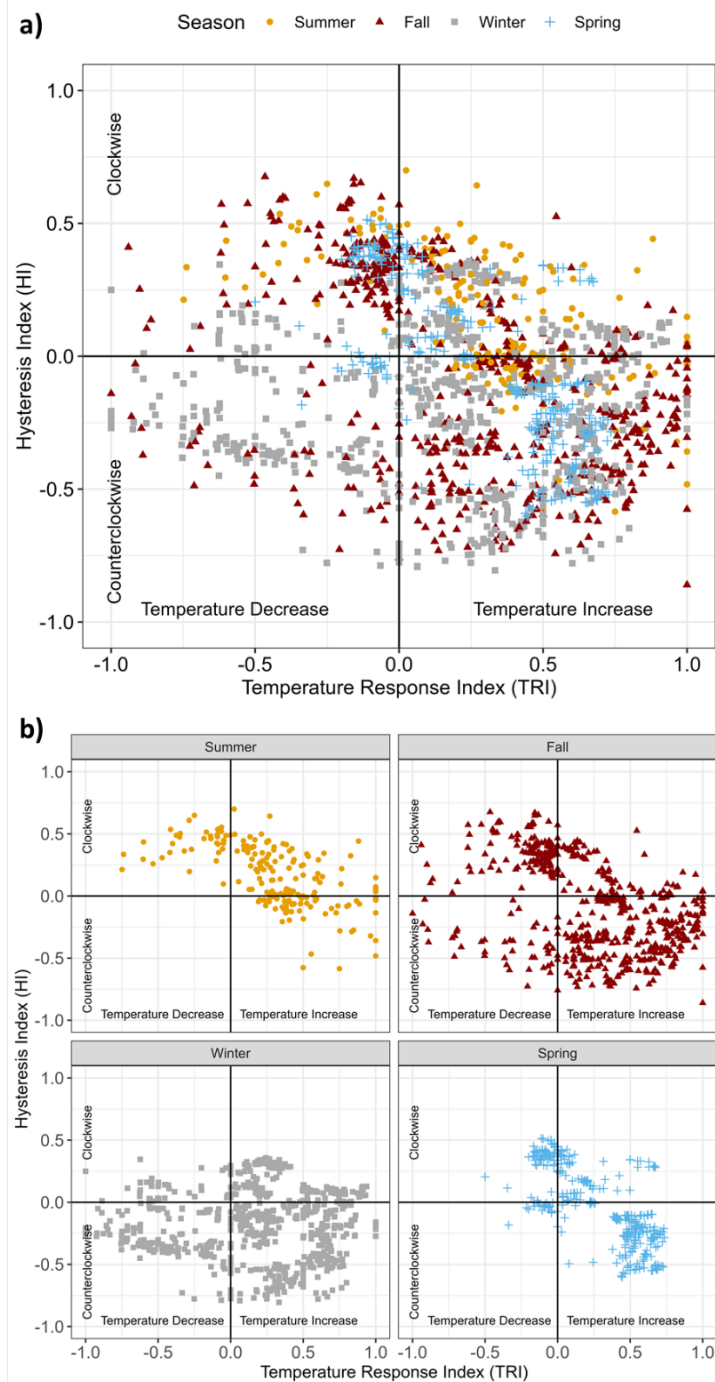


FIGURE 2 (a) Overall seasonal pattern of hysteresis (HI) and temperature response index (TRI) indices and (b) seasonal pattern illustrating the variability of the relationship between these indices per storm event.

The post-hoc multiple comparisons test provided strong evidence that median HI values across all 10 catchments were different among all seasonal combinations per catchment (Table S4). Median HI values for summer events were 0.15 ± 0.23 (SD) but decreased substantially in fall (-0.03 ± 0.36) and winter (-0.16 ± 0.26). During spring events, the median HI was close to zero but the standard deviation was high (-0.04 ± 0.28). Negative HI values occurred in the beginning of the spring season (early April storm events) and progressed to positive hysteresis from early May to the end of the season, resulting in an overall positive average spring HI weighted by stream (Table 2).

TABLE 2 Median and standard deviation (SD) of the hysteresis index (HI) and temperature response index (TRI) by season for the five study streams in each of the two sub-regions.

Statistic	Season	Tectah					McGarvey					Overall median	Overall average
		Stream ID											
		1	2	3	4	5	11	13	14	15	18		
Hysteresis index (HI)	Summer	0.00	-0.01	-0.02	0.17	0.03	0.12	0.25	0.20	0.22	0.28	0.15	0.13
	Fall	0.00	-0.31	-0.25	-0.12	-0.03	-0.57	0.34	0.19	-0.02	-0.02	-0.03	-0.07
	Winter	-0.02	-0.19	-0.26	-0.10	0.14	-0.30	-0.27	-0.33	-0.06	-0.13	-0.16	-0.15
	Spring	-0.20	0.00	-0.05	0.03	0.29	0.11	-	-0.04	-0.05	-0.12	-0.04	-0.01
HI SD	Summer	0.27	0.20	0.27	0.22	0.24	0.33	0.41	0.22	0.21	0.14	0.23	0.25
	Fall	0.28	0.35	0.29	0.38	0.32	0.42	0.44	0.40	0.29	0.42	0.36	0.36
	Winter	0.20	0.31	0.24	0.31	0.36	0.20	0.27	0.37	0.24	0.20	0.26	0.27
	Spring	0.34	0.29	0.35	0.34	0.25	0.28	-	0.27	0.21	0.28	0.28	0.29
Temperature response index (TRI)	Summer	0.45	0.27	0.38	0.33	0.30	0.40	-0.48	0.46	0.27	0.25	0.31	0.27
	Fall	0.27	0.35	0.37	0.24	0.32	0.34	-0.28	-0.17	0.30	-0.07	0.29	0.18
	Winter	0.30	0.52	0.33	0.25	0.17	0.14	-0.27	0.06	0.04	0.10	0.16	0.16
	Spring	0.49	0.23	0.27	0.32	0.55	0.29	-	0.07	0.24	0.08	0.27	0.28
TRI SD	Summer	0.28	0.11	0.30	0.24	0.32	0.27	0.66	0.59	0.24	0.44	0.29	0.34
	Fall	0.44	0.41	0.47	0.34	0.42	0.36	0.46	0.52	0.18	0.38	0.42	0.40
	Winter	0.46	0.46	0.27	0.48	0.13	0.54	0.52	0.23	0.42	0.49	0.46	0.40
	Spring	0.30	0.31	0.25	0.31	0.32	0.28	-	0.29	0.29	0.31	0.30	0.30

TRI values were consistently positive in almost all streams across all seasons. The exceptions, where storm events resulted in negative temperature response patterns or a decrease in temperature, occurred in stream 13 during all seasons, and streams 14 and 18 during fall (Figure 2b). The consistently positive TRI values in most streams are indicative of increasing

stream temperatures on the rising limb of the storm hydrograph. While generally positive, seasonal TRI values tended to be greatest during summer events, followed by fall, spring, then winter (Table 2). Uniquely, TRI values for stream 13 located in the McGarvey watershed were strongly negative during summer, fall, and winter, indicating stream cooling on the rising limb of events. Across all streams per catchment, there was no statistical evidence that TRI values were different across seasons in Tectah, and between spring and summer in McGarvey (Table S4). A post-hoc multiple comparisons test provided suggestive evidence of a weak seasonal median TRI difference between summer and fall (Dunn's test statistic $[Z] = -2.26$; $p = 0.071$) and strong evidence of a difference in TRI between summer and winter ($Z = 2.91.65$; $p = 0.021$).

Catchments exhibited a similar seasonal hysteresis and temperature response patterns in stream temperature across both Tectah and McGarvey sub-regions (Figure S11). In general, clockwise hysteresis was more predominant during spring and summer events and counterclockwise hysteresis was more likely during fall and winter events.

Average T_s varied per catchment being generally warmer in McGarvey (Figure 3a – left). Stream temperatures in Tectah and McGarvey were warmest during the summer followed by the spring events. In the McGarvey streams, the T_s patterns were generally distinct among seasons, with no evidence of differences in T_s between fall and spring (Table S5 - $Z = -0.743$; $p = 0.457$). Additionally, the mean difference in T_s in the McGarvey streams was small between summer and fall ($Z = -11.01$; $p < 0.001$) and between fall and spring ($Z = -0.743$; $p < 0.001$) when compared to Tectah ($Z = -15.34$ (summer and fall) and 5.68 (fall and spring); $p < 0.0001$ for both seasonal combinations). We also evaluated the seasonal patterns in peak stage and the hysteresis indices per storm event (Figure 3a – right). Peak stage varied among seasons for the streams. However, peak stage in McGarvey was generally greater during (a) summer and fall and (b) had greater

variability during winter compared to Tectah. Peak stage values in McGarvey during summer and spring did not differ statistically (Table S5: $Z = 0.53$; $p = 0.59$). For Tectah, spring and fall stream stage were also not statistically different ($Z = -0.238$; $p = 0.812$). In general, Tectah streams average peak stage displayed a progression from low to high values between summer and winter, a pattern observed in the average peak stage of McGarvey streams. We also evaluated how average T_s and peak stage varies with HI (Figure 3b). For Tectah streams, clockwise hysteresis was more frequent as average T_s increased and peak stage decreased seasonally. The same was observed for McGarvey streams, but with more variability in HI values and higher seasonal average T_s compared to Tectah. In general, the relationship between HI and average T_s / peak stage was less linear as the seasons progressed in McGarvey. These results indicate that HI, T_s , and stream stage patterns in these two main regions may be driven by distinct catchment and storm processes, such as subsurface flow, groundwater interactions, and both intensity and duration of storm events.

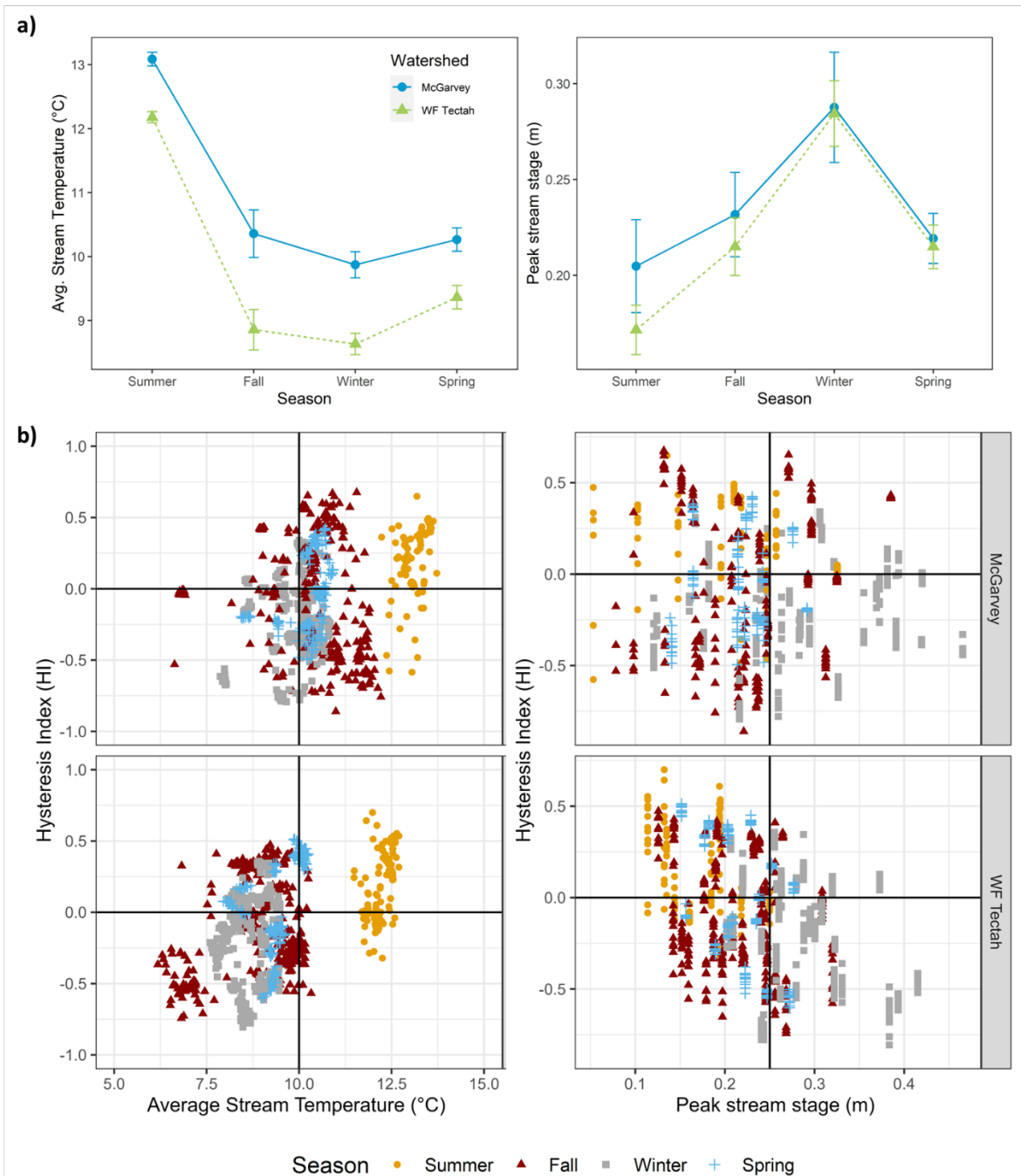


FIGURE 3 Median average stream temperature (°C; a - left) and median peak stream stage (m; a - right) interaction plots based on Dunn's Test for multiple comparisons, and the seasonal hysteresis indices compared to the average stream temperature (b-left) and the peak stream stage values per storm event per watershed (b - right).

3.2. Clustering

We explored the mechanisms influencing the T_s hysteretic behavior using clustering analysis. We initiated the analysis with $k = 2$ because of a potential distinction in HI and TRI relationship by catchment. The silhouette and the Jaccard similarities stability tests indicated that two clusters produced the most stable results with the least amount of overlap area between the clusters (Figure 4a). The BSS/TSS ratio was 12.9 % and the total within-cluster sum of squares was approximately 81,000. Jaccard results indicated that both clusters 1 ($J = 0.89$) and 2 ($J = 0.91$) were highly stable. Statistical analysis of the 51 variables in each cluster provided evidence that there were differences between the initial stream stage (m), the storm depth (mm), storm duration (hr), and wetted width (m), but there were no differences between the standard deviation of flow weighted slope (%) per cluster. These results showed that the overall variability in hysteresis was mainly driven by meteorological characteristics of the storms, principally the peak air temperatures and the gradient between stream and air temperatures in the rising limb of the storms (Figures S12).

Although there was some overlap between clusters (Figure 4a), we found an indication that the clusters differed across watersheds in terms of HI and TRI. When comparing the scaled values of each variable per cluster, cluster 1 had the lowest median HI value and the greatest variability in meteorological characteristics (e.g., initial stream stage (m), storm depth (mm), and storm duration (hr); Figure 4b). In contrast, cluster 2 had the greatest median TRI and a wider distribution of values associated with topographic variables, such as flow weighted slope (Figure S12). These results indicate that the hysteretic response of stream temperature to rain events, as described by the HI values, was strongly related to catchment characteristics. Our analysis also

demonstrated that the contrast in T_s and stream stage patterns per cluster was likely driven by topographic and meteorological characteristics of each catchment.

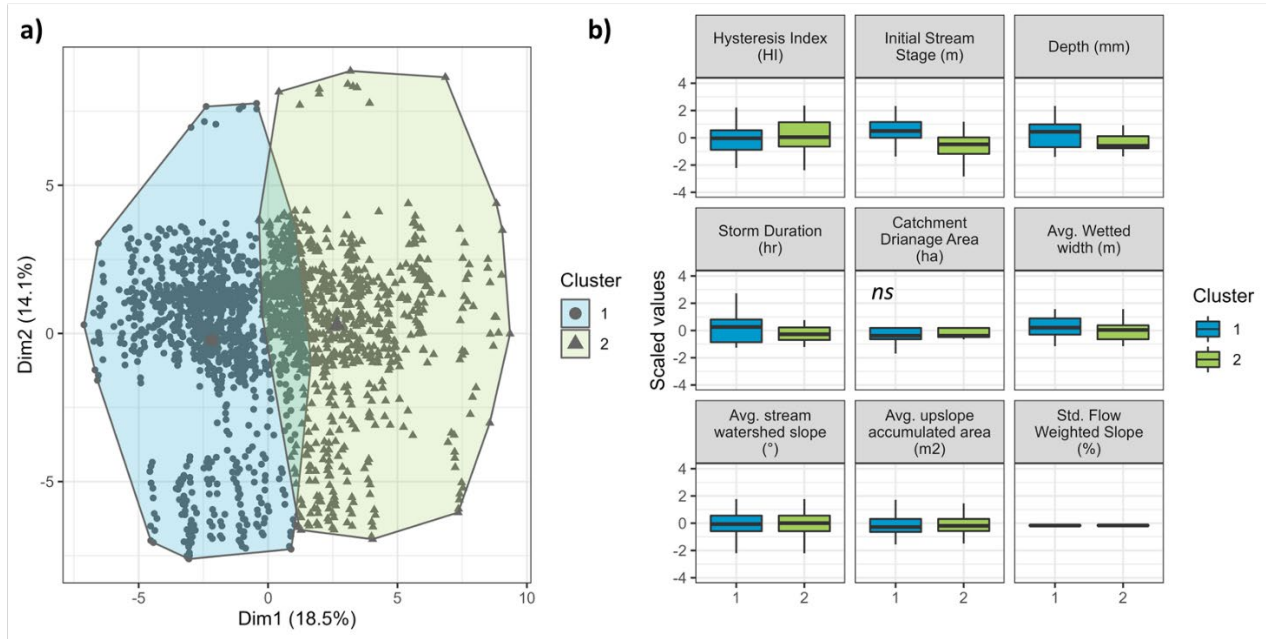


FIGURE 4 Results for (a) the overall k -means clustering analysis and (b) the boxplots of main scaled input variables per cluster (*ns*: median of clusters not significantly different at 0.05 level). X and Y coordinates in (a) represent the two most representative principal components from the linear combinations of the original data.

Overlapping of clusters is a known issue in clustering analysis— occur due to noise, features are not capturing all necessary information, or it may be inherent to the processes that produced the data (Adam and Blockeel, 2015). We observed a partial overlap between clusters 1 and 2 in the previous analysis. As such, we also analyzed the sub-regions, McGarvey and Tectah, independently using cluster analysis to avoid uncertainties associated with cluster overlap, identify the potential number of clusters formed, their stability, and the regional hysteretic response based on the meteorological and topographic characteristics. This analysis increased

BSS/TSS ratio (previously 12.9 %) by 3.8 % for McGarvey and 1.8 % for Tectah, and decreased the total within-cluster sum of squares (previously ~81,000) by more than 55 % for McGarvey and ~ 44 % for Tectah. Although the BSS/TSS ratio was not close to one for any of the clustering results in this study, the Jaccard similarities cluster stability assessment resulted in relatively stable clusters for both overall and individual catchment analysis. The mean of Jaccard bootstrap coefficient for clusters formed in the McGarvey analysis were approximately 0.57 and 0.59, while for Tectah these coefficients reached almost 1 (Cluster 1 $J = 0.92$; Cluster 2 $J = 0.91$).

The cluster analysis of streams in the McGarvey sub-region also demonstrated that the hysteretic behavior of stream temperature was likely driven by the topographic characteristics of the catchments (Figure 5 - top). For instance, while the hysteretic behavior of T_s significantly differed per cluster in McGarvey, the distributions of storm characteristics (meteorological variables), such as depth (mm), duration (hours), average rainfall intensity (mm/hr), and mean daily solar radiation ($W/m^2/day$) were not statistically different (Figure 5b - top). Comparatively, our results revealed a consistent variability in HI values associated with variability in topographic characteristics (Figure S13). As an example, the cluster with the largest variability in HI values (Figure 5 - top, cluster 1) also had the greatest variability in elevation, average catchment slope, and topographic wetness index.

Interestingly, the cluster analysis of the data from the Tectah sub-region suggested that the stream temperature hysteretic behavior was most strongly related to the meteorological characteristics of the region (Figure 5 – bottom). For instance, the cluster with the greatest HI distribution (cluster 1) was associated with lower antecedent rainfall, higher maximum 1-hour rainfall intensity, greater solar radiation, and greater air temperature (Figure 5b – bottom). The

magnitude of these meteorological components significantly differed between the two clusters. Cluster 2 consisted predominantly of counterclockwise T_s hysteretic behavior, likely driven by the higher antecedent moisture and incidence of solar radiation in the system. There was no evidence of a relationship between T_s hysteretic behavior and topographic characteristics in Tectah. This was interesting given there was evidence that physiological characteristics, such as slope and elevation, were statistically different across our study watersheds. However, the difference in the variability of the meteorological variables between clusters was greater and, therefore, a likely stronger driver of the hysteretic response in the Tectah catchments (Figure S14).

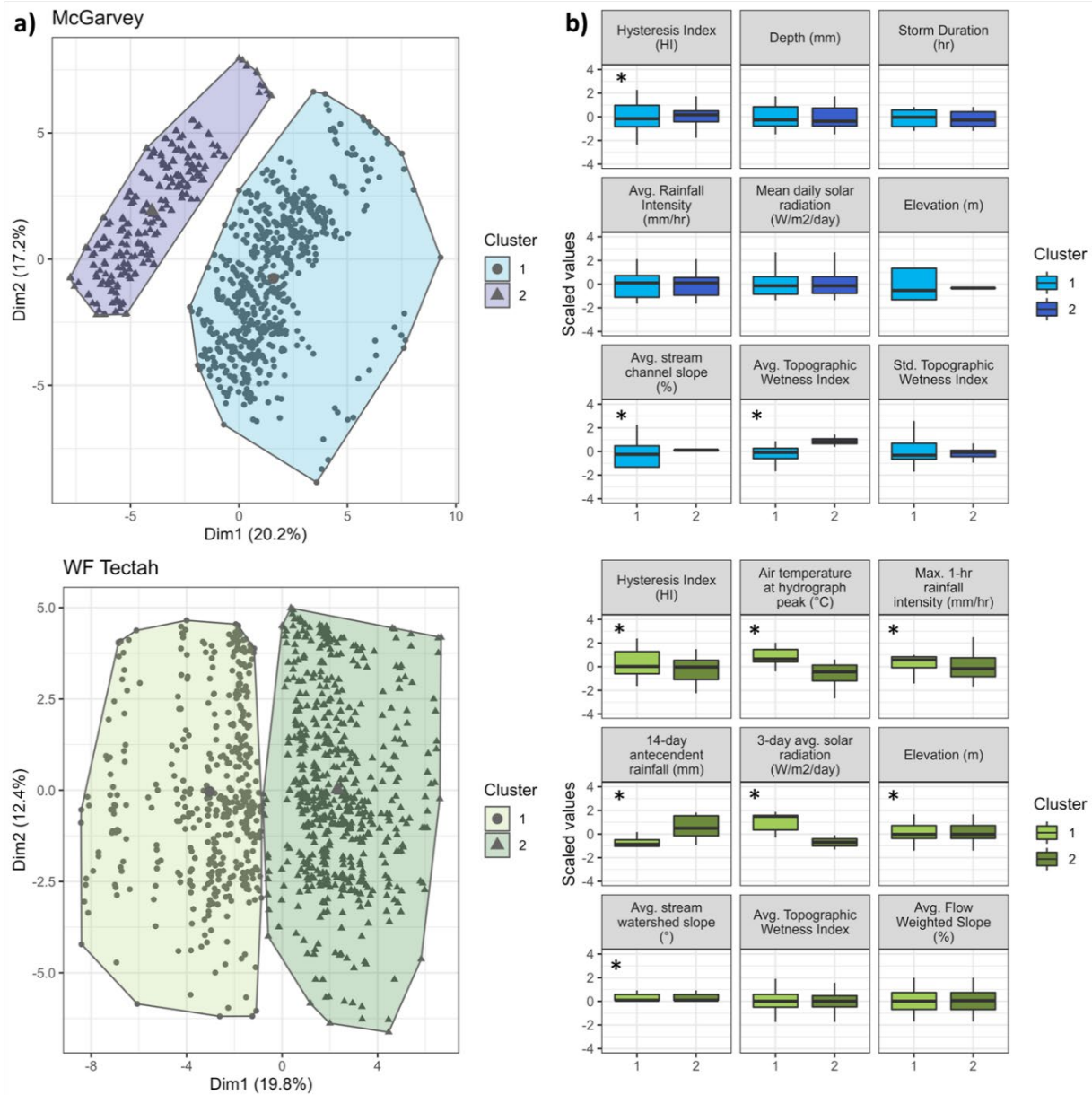


FIGURE 5 Results for (a) McGarvey (top) and Tectah (bottom) *k*-means clustering analysis and (b) the boxplots of each scaled input variable per cluster per catchment (*: medians of the clusters were significantly different at 0.05 level). X and Y coordinates in (a) represent the two most representative principal components from the linear combinations of the original data.

We compared the difference per variable between the clusters in McGarvey and Tectah (Figure 6). Our results indicated that the distribution of all meteorological variables was significantly different per cluster in Tectah (p -value < 0.05). However, only nine of these variables varied significantly per cluster in McGarvey. Our results suggested that the significant variation in T_s hysteresis previously observed in McGarvey (Figure 5 - top) was highly associated with the variability of each topographic variable. Only four of the topographic variables (i.e., average stream channel slope (%), wetted width at each monitoring location (m), elevation (m)) were relevant for the distinct patterns in hysteresis per cluster in Tectah streams.

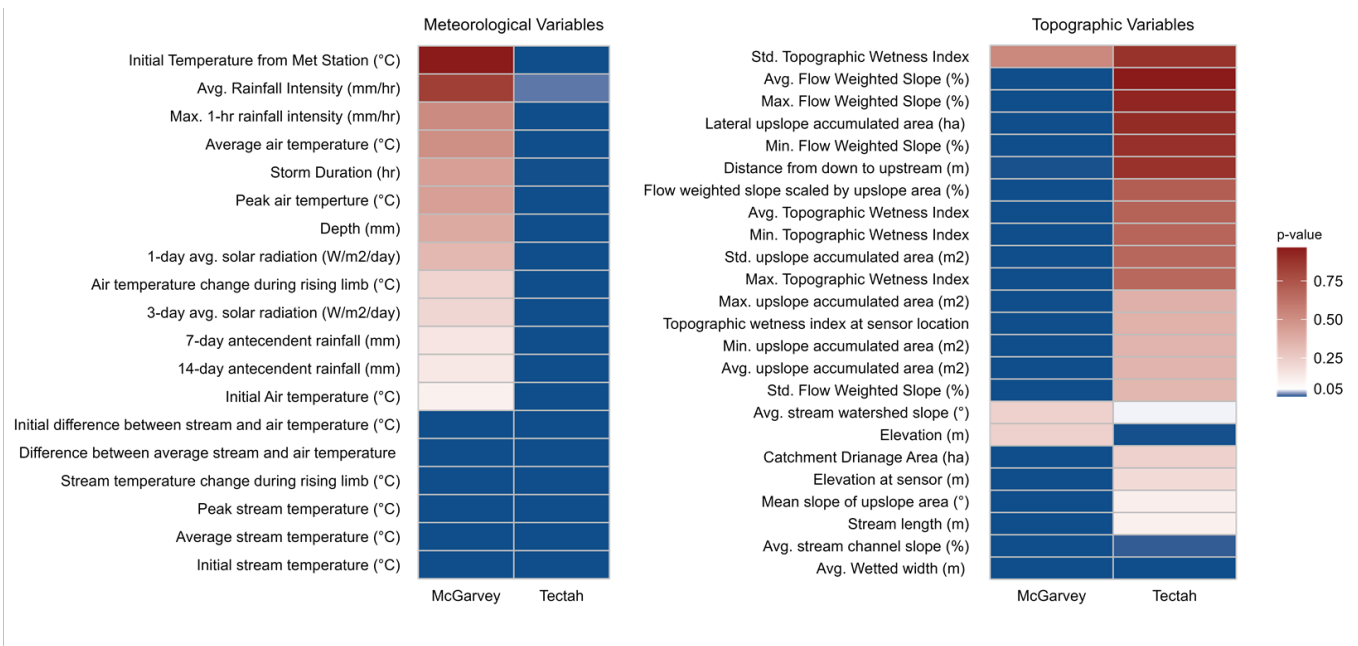


FIGURE 6 Heatmaps of p -values (Kruskal-Wallis) for tests analyzing the differences in meteorological (left) and topographic (right) variables between the clusters identified in our clustering analysis.

4. DISCUSSION

Accepted Article

In our study of 10 streams in Northern California, we observed a seasonally variable relationship between stream temperature (T_s) and stormflow, with clockwise hysteresis occurring during spring and summer and counterclockwise hysteresis occurring during fall and winter storm events. During spring and summer, T_s warmed on the rising limb and cooled on the falling limb of the storm hydrograph. There are a couple plausible explanations for this phenomenon, which occurred during seasons when stream temperature is generally cooler than air temperature. For example, clockwise hysteretic behavior may have occurred due to heat availability in the catchment during the days preceding precipitation events, which was then flushed via advection into the streams during the initial onset of precipitation (Kobayashi et al., 1999; Wilby et al., 2014). This initial warming during summer and spring storm events is consistent with mechanisms of groundwater ridging where accumulated warm water within the narrow riparian zone or permanent saturated areas could be rapidly discharged into streams at the onset of precipitation events (e.g., Sklash and Farvolden, 1979). The temperature response index (TRI) values were also consistent with this theory as they were generally positive and indicative of heat inputs to the stream during the rising limb. Seasonally, TRI median values were highest in summer, decreased through the wet season, and increased during spring. However, it is also possible that precipitation events led to greater contributions of groundwater to streams on the falling limb as flow paths interconnected (Kobayashi et al., 1999; Subehi et al., 2010), resulting in discharge of cooler groundwater to the streams later in the events (Lange and Haensler, 2012).

During fall and winter, when hydrologic connectivity was greatest and air temperatures were cooler than stream temperatures, the counterclockwise hysteresis indicated that stream temperatures were cooler on the rising limb and warmer on the falling limb of the storm hydrograph. This pattern is potentially explained by the contribution of deep groundwater flow

Accepted Article

paths that input comparatively warm groundwater (Kobayashi et al., 1999; Lange and Haensler, 2012). If we assume that deep groundwater temperatures can be approximated by adding 1–2 °C to mean annual air temperatures (Ficklin et al., 2012; Leach and Moore, 2015), then deep groundwater temperatures may be within the range of 12–13 °C for this Northern California region. Input of groundwater in this temperature range during the falling limb of all the observed fall and winter storm events would cause stream warming and provide evidence for the counterclockwise behavior observed herein. This groundwater interaction is likely evident in McGarvey streams, where average T_s was higher compared to Tectah streams, and where the topographic mechanisms are potential controls of the hysteretic behavior observed. Counterclockwise behavior may also be a result of direct rainfall into the channel and throughflow from adjacent hillslopes, such as those derived from longer flow paths that do not activate until later in the storm event when full hillslope-riparian-stream connectivity is achieved (Penna et al., 2015; Uchida et al., 2002; H. J. Van Meerveld et al., 2015). Indeed, during times of maximum hydrologic connectivity preferential flow paths can deliver groundwater from upper hillslopes that influence stream temperatures (Uchida et al., 2002). It is likely that for storms during the wettest part of the year, subsurface water is sufficiently mixed prior to emerging in the stream that these lateral inputs can cause localized warming.

Other studies have observed similar T_s hysteresis behavior. Kobayashi et al (1999) paired stream temperature and specific conductance measurements and observed clockwise stream temperature hysteresis during an early fall storm, while specific conductance exhibited counterclockwise hysteresis. The authors suggested that inputs of shallow subsurface flow on the rising limb warmed through the soil increasing T_s , and simultaneously diluted specific conductance in the stream. After the storm peak, specific conductance increased and stream

temperature decreased, indicating that the contributions from shallow sources decreased and inputs from deeper groundwater cooled the stream. This may have been the mechanism causing stream warming (positive TRI values) during summer and spring events in our streams.

However, it does not explain why temperatures increased on the rising limb during fall and winter for both Tectah and McGarvey. Subehi et al (2010) observed seasonally variable stream temperature hysteresis across 16 forested watersheds (0.5 to 100 ha) in Japan, with clockwise hysteresis during spring and summer seasons and counterclockwise hysteresis during fall and winter, which is similar to the trend observed herein. The authors conclude that watershed slope and the magnitude of streamflow change during storm events had a greater effect on stream temperature change during storm events than air temperature change. In our study, slope was a significant mechanism in the detection of stable clusters for both McGarvey and Tectah streams. While air temperature was not significant per cluster in McGarvey, channel slope variability appeared to most influence its T_s hysteretic behavior.

We acknowledge the variability in HI and TRI values per stream, which may be a result of several processes. The longitudinal variability in HI and TRI values was greatest during the summer and fall and decreased during winter and spring. This is likely because low flows in the late summer lead to greater longitudinal thermal heterogeneity than during wetter portions of the year (Leach et al., 2016), where stream temperature may be dominated by discrete groundwater sources or hyporheic exchange that buffers the response to storm flow (Leach et al., 2017; Lowry et al., 2007). Once groundwater levels began to rise during the onset of the wet season and watershed storage thresholds became satisfied (e.g., (Detty and McGuire, 2010), stream temperatures along these streams became more homogeneous, and more synchronous in their response to storm flow. At the same time, runoff generation during events likely shifts from

shallow subsurface sources to deeper, longer groundwater flow paths that are now connected (Lange and Haensler, 2012). This behavior could also be explained by differences in the dominate energy exchanges influencing stream temperature change between summer and winter. Future research should focus on data of covariates (e.g., site-specific soil water content, groundwater) to help explain the HI and TRI variability found in this study.

In McGarvey streams, the hysteresis gradient observed per cluster appeared to be mostly driven by surface topography metrics such as average stream channel slope (*avg_ch_slope*), wetted width in meters (*avg_act_wd*), FWS, TWI, and UAA (Figure S13). Those stream bed and channel characteristics are indicative of hyporheic exchanges (Poole et al., 2001) or the transfer of water between the stream and the saturated bed or riparian zone. This transfer may occur principally in streams with marked changes in gradient such as the step-pool system streams in McGarvey (Moore et al., 2005). Our results also revealed a relatively higher average T_s pattern throughout seasons in McGarvey compared to Tectah. This may indicate a hillslope and groundwater dominated system, where deep groundwater is typically warmer than stream water, potentially causing stream warming (Bogan et al., 2003). McGarvey, located close to the ocean, is also a region considerably influenced by coastal fog. The formation of fog, which reduces the natural heat exchange between the stream and the atmosphere (Caissie, 2006), is an important source of moisture during the summer (Dawson, 1998) and may promote a homogenous stream thermal regime in this region, principally throughout fall and spring seasons when we found no evidence of difference among T_s values.

In Tectah, during both warm and cool seasons, the direction of hysteresis appeared to be mainly driven by the gradient between stream and air temperatures, antecedent rainfall events, solar radiation, and direction of air temperature change during events. This is similar to recent

work, where Oware and Peterson (2020) measured seasonally variable thermal gradients during storm events, with stream and hyporheic substrate temperatures increasing during summer storms and decreasing during winter storms. During warm season storm events, when the direction of the thermal gradient is from the air to the stream, T_s initially increased resulting in clockwise hysteresis. In Tectah streams, the thermal gradient between stream and air temperatures ($ts_ta_dif_i$ – Figure S14) was significantly different per cluster and followed the HI cluster patterns, indicating that the magnitude of T_s hysteresis was largest during events with the largest temperature gradient between the stream and overlying air. If we assume air temperatures approximate rainfall temperatures (Gerecht, 2012; Shanley and Peters, 1988), this indicates transfer of heat from rainfall through soil to stream, likely via shallow subsurface inputs and direct channel interception. In addition, the cluster pattern of air temperature change during the event (ta_rl_r – Figure S14) showed an opposite relationship with HI, indicating that stream temperatures generally reflected the direction of air temperature change during storm events (e.g., stream temperatures warmed (cooled) when air temperatures warmed (cooled)).

This study has a few important limitations. The use of single point precipitation measurements on two adjacent ridges likely resulted in under characterization of the in-stream temperature response to precipitation, as single point precipitation measurements are known to cause error when extrapolated across entire catchments (Croghan et al., 2019). Although storm characteristics were not found to be meaningfully different between rain gauge locations, catchment-scale differences in vegetation likely influenced the amount of hydrologic input driving stormflow, but vegetation type was not accounted for in this study. In addition, measurement of rainfall water temperature and soil moisture would have been valuable to understand whether the observed hysteresis was due to variable subsurface flow paths

(Kobayashi et al., 1999) or whether stream temperature fluctuations during storm events was simply a reflection of rainfall temperature, especially for events early in the wet season when shallow subsurface pathways likely dominated. As well, hysteresis metrics for each stream temperature monitoring location were calculated using the same time series as stream stage, which was measured at the downstream catchment outlet. This likely provided a reasonable estimate of the streamflow response at each stream temperature measurement point because of the small area of the study catchments and relatively short stream reaches. Despite this assumption, installation of additional level loggers and additional measurements of stream discharge along each study reach may have provided more accurate calculation of these metrics, and may have provided a better explanation of the variability in hysteretic behavior along each stream. Future work should also include spatially distributed measurements of soil temperature at a range of depths and groundwater levels to further elucidate variable runoff generation mechanisms using stream temperature as a tracer and provide additional evidence that metrics describing the hysteresis of stream temperature during storm events correlate well to measurements upslope. Additional analysis is required to determine whether hysteresis metrics using stream temperature and stormflow could be used to assess the influence of forest harvesting or other disturbances on stream flow response, potentially providing an additional method of quantifying the effects of reach scale perturbations on hydrologic processes in forested headwaters (e.g., Mistick and Johnson, 2020).

5. CONCLUSIONS

We evaluated the seasonal stream temperature response to stormflow across 23 storm events and 10 forested headwater catchments outfitted with spatially distributed stream

temperature sensors in the Northern California coast range during the 2020 water year. We used hysteresis metrics to quantify the magnitude and direction of stream temperature change and used clustering analysis to assess what meteorological, hydrological, and topographic characteristics influence stream temperature change during storm events. Our results indicate that the stream temperature response to stormflow is seasonally variable and exhibits clockwise hysteresis during spring and summer and counterclockwise hysteresis during fall and winter. Overall the hysteretic response was highly intertwined to the unique characteristics of each catchment. Although variables such as the gradient between stream and air temperatures at the start of the event, slope, wetted width, and elevation were all important in the distinct hysteretic patterns observed per sub-region clusters. The magnitude and direction of stream temperature hysteresis in Tectah was well associated with antecedent rainfall, solar radiation, rainfall intensity, and air temperature change during the storm rising limb, indicating the role of regional meteorological conditions on stream temperature change during storm events. For McGarvey, the magnitude and direction of T_s hysteresis were most intertwined to the surface topography characteristics of the channel and the streambed, indicating the role of hillslope characteristics and potential groundwater interactions on stream temperature changes during storms in headwater streams. Future research should consider a detailed assessment of groundwater contributions to forest headwaters thermal regimes while accounting for changes in watershed microclimate and disturbance.

ACKNOWLEDGEMENTS

We thank Matt House and Drew Coe for facilitating development of the research ideas and selection of field sites. We are also grateful for the efforts of Matt Nannizzi, Pat Righter,

Jonah Nicholas, Sam Zamudio, Cedric Pimont, and Katie Wampler for their assistance installing field equipment and collecting data. This research was funded by the California Board of Forestry and Fire Protection Effectiveness Monitoring Committee, grant number 9CA04452.

ORCID

Lorrayne Miralha 0000-0003-1448-9321

Austin Wissler 0000-0001-8368-0053

Catalina Segura 0000-0002-0924-1172

Kevin D. Bladon 0000-0002-4182-6883

REFERENCES

- Aguilera, R., Melack, J.M., 2018. Concentration-Discharge Responses to Storm Events in Coastal California Watersheds. *Water Resour. Res.* 54, 407–424. <https://doi.org/10.1002/2017WR021578>
- Amatya, D.M., Campbell, J.L., Wohlgemuth, P., Elder, K.J., Sebestyen, S., Johnson, S.L., Keppeler, E.T., Adams, M.B., Caldwell, P., Misra, D., 2016. Hydrological processes of reference watersheds in experimental forests, USA, in: Amatya, D.M., Williams, T.M., Bren, L., Jong, C. (Eds.), *Forest Hydrology: Processes, Management and Assessment*. CABI, Boston, MA, USA, pp. 227–227. <https://doi.org/10.1079/9781780646602.0000>
- Aytaç, E., 2020. Unsupervised learning approach in defining the similarity of catchments: Hydrological response unit based k-means clustering, a demonstration on Western Black Sea Region of Turkey. *Int. Soil Water Conserv. Res.* 8, 321–331. <https://doi.org/10.1016/j.iswcr.2020.05.002>
- Beven, K.J., Kirkby, M.J., 1979. A physically based, variable contributing area model of basin hydrology / Un modèle à base physique de zone d'appel variable de l'hydrologie du bassin versant. *Hydrol. Sci. Bull.* 24, 43–69. <https://doi.org/10.1080/02626667909491834>
- Blaen, P.J., Hannah, D.M., Brown, L.E., Milner, A.M., 2013. Water temperature dynamics in High Arctic river basins. *Hydrol. Process.* 27, 2958–2972. <https://doi.org/10.1002/hyp.9431>
- Bogan, T., Mohseni, O., Stefan, H.G., 2003. Stream temperature-equilibrium temperature relationship. *Water Resour. Res.* 39.
- Brewitt, K.S., Danner, E.M., Moore, J.W., 2017. Hot eats and cool creeks: Juvenile Pacific Salmonids use mainstem prey while in thermal refuges. *Can. J. Fish. Aquat. Sci.* 74, 1588–1602. <https://doi.org/10.1139/cjfas-2016-0395>
- Briggs, M.A., Lane, J.W., Snyder, C.D., White, E.A., Johnson, Z.C., Nelms, D.L., Hitt, N.P., 2018. Shallow bedrock limits groundwater seepage-based headwater climate refugia. *Limnologia* 68, 142–156. <https://doi.org/10.1016/j.limno.2017.02.005>
- Briggs, M.A., Lutz, L.K., McKenzie, J.M., Gordon, R.P., Hare, D.K., 2012. Using high-resolution distributed temperature sensing to quantify spatial and temporal variability in vertical hyporheic flux. *Water Resour. Res.* 48, 1–16. <https://doi.org/10.1029/2011WR011227>
- Butturini, A., Alvarez, M., Bernal, S., Vazquez, E., Sabater, F., 2008. Diversity and temporal sequences of forms of DOC and NO₃- discharge responses in an intermittent stream: Predictable or random succession? *J. Geophys. Res. Biogeosciences* 113, 1–10. <https://doi.org/10.1029/2008JG000721>
- Caissie, D., 2006. The thermal regime of rivers: A review. *Freshw. Biol.* 51, 1389–1406. <https://doi.org/10.1111/j.1365-2427.2006.01597.x>
- Callahan, M.K., Rains, M.C., Bellino, J.C., Walker, C.M., Baird, S.J., Whigham, D.F., King, R.S., 2015. Controls on temperature in salmonid-bearing headwater streams in two common hydrogeologic settings, Kenai Peninsula, Alaska. *J. Am. Water Resour. Assoc.* 51, 84–98. <https://doi.org/10.1111/jawr.12235>
- Croghan, D., Van Loon, A.F., Sadler, J.P., Bradley, C., Hannah, D.M., 2019. Prediction of river temperature surges is dependent on precipitation method. *Hydrol. Process.* 33, 144–159. <https://doi.org/10.1002/hyp.13317>
- Dawson, T.E., 1998. Fog in the California redwood forest: ecosystem inputs and use by plants. *Oecologia* 117, 476–485. <https://doi.org/10.1007/s004420050683>

- Demars, B.O. I., Russell Manson, J., Ólafsson, J.S., Gíslason, G.M., Gudmundsdóttir, R., Woodward, G., Reiss, J., Pichler, D.E., Rasmussen, J.J., Friberg, N., 2011. Temperature and the metabolic balance of streams. *Freshw. Biol.* 56, 1106–1121. <https://doi.org/10.1111/j.1365-2427.2010.02554.x>
- Detty, J.M., McGuire, K.J., 2010. Threshold changes in storm runoff generation at a till-mantled headwater catchment. *Water Resour. Res.* 46, 1–15. <https://doi.org/10.1029/2009WR008102>
- Dralle, D.N., Hahm, W.J., Rempe, D.M., Karst, N.J., Thompson, S.E., Dietrich, W.E., 2018. Quantification of the seasonal hillslope water storage that does not drive streamflow. *Hydrol. Process.* 32, 1978–1992. <https://doi.org/10.1002/hyp.11627>
- Driscoll, E.D., Palhegyi, G.E., Strecker, E.W., Shelley, P.E., 1989. Analysis of Storm Event Characteristics for Selected Rainfall Gages Throughout the United States: Draft. U.S. Environmental Protection Agency.
- Dunn, O.J., 1964. Multiple Comparisons Using Rank Sums. *Technometrics* 6, 241–252. <https://doi.org/10.1080/00401706.1964.10490181>
- Erdozain, M., Emilson, C.E., Kreutzweiser, D.P., Kidd, K.A., Mykytczuk, N., Sibley, P.K., 2020. Forest management influences the effects of streamside wet areas on stream ecosystems. *Ecol. Appl.* 30, 1–16. <https://doi.org/10.1002/eap.2077>
- Evans, C., Davies, T.D., 1998. Causes of concentration/discharge hysteresis and its potential as a tool for analysis of episode hydrochemistry. *Water Resour. Res.* 34, 129–137. <https://doi.org/10.1029/97WR01881>
- Fellman, J.B., Hood, E., Dryer, W., Pyare, S., 2015. Stream physical characteristics impact habitat quality for pacific salmon in two temperate coastal watersheds. *PLoS ONE* 10, 1–16. <https://doi.org/10.1371/journal.pone.0132652>
- Fellman, J.B., Nagorski, S., Pyare, S., Vermilyea, A.W., Scott, D., Hood, E., 2014. Stream temperature response to variable glacier coverage in coastal watersheds of Southeast Alaska: STREAM TEMPERATURE RESPONSE TO VARIABLE GLACIER COVERAGE. *Hydrol. Process.* 28, 2062–2073. <https://doi.org/10.1002/hyp.9742>
- Ficklin, D.L., Luo, Y., Stewart, I.T., Maurer, E.P., 2012. Development and application of a hydroclimatological stream temperature model within the Soil and Water Assessment Tool. *Water Resour. Res.* 48, 1511. <https://doi.org/10.1029/2011WR011256>
- Freeman, M.C., Pringle, C.M., Jackson, C.R., 2007. Hydrologic connectivity and the contribution of stream headwaters to ecological integrity at regional scales. *J. Am. Water Resour. Assoc.* 43, 5–14. <https://doi.org/10.1111/j.1752-1688.2007.00002.x>
- Freer, J., McDonnell, J.J., Beven, K.J., Peters, N.E., Burns, D.A., Hooper, R.P., Aulenbach, B., Kendall, C., 2002. The role of bedrock topography on subsurface storm flow. *Water Resour. Res.* 38, 1–16. <https://doi.org/10.1029/2001wr000872>
- Gabrielli, C.P., McDonnell, J.J., Jarvis, W.T., 2012. The role of bedrock groundwater in rainfall-runoff response at hillslope and catchment scales. *J. Hydrol.* 450–451, 117–133. <https://doi.org/10.1016/j.jhydrol.2012.05.023>
- Genereux, D.P., Hemond, H.F., Mulholland, P.J., 1993. Spatial and temporal variability in streamflow generation on the West Fork of Walker Branch Watershed. *J. Hydrol.* 142, 137–166. [https://doi.org/10.1016/0022-1694\(93\)90009-X](https://doi.org/10.1016/0022-1694(93)90009-X)
- Gerecht, K., 2012. Anomalous stream temperature response to storms in a forested headwater stream in Central Pennsylvania. Pennsylvania State University.

- Gomi, T., Asano, Y., Uchida, T., Onda, Y., Sidle, R.C., Miyata, S., Kosugi, K., Mizugaki, S., Fukuyama, T., Fukushima, T., 2010. Evaluation of storm runoff pathways in steep nested catchments draining a Japanese cypress forest in central Japan: a geochemical approach. *hydrological* 24, 550–566. <https://doi.org/10.1002/hyp.7550>
- Hangen, E., Lindenlaub, M., Leibundgut, C., Von Wilpert, K., 2001. Investigating mechanisms of stormflow generation by natural tracers and hydrometric data: A small catchment study in the Black Forest, Germany. *Hydrol. Process.* 15, 183–199. <https://doi.org/10.1002/hyp.142>
- Hartigan, J.A., Wong, M.A., 1979. Algorithm AS 136: A K-Means Clustering Algorithm. *J. R. Stat. Soc. Ser. C Appl. Stat.* 28, 100–108. <https://doi.org/10.2307/2346830>
- Hebert, C., Caissie, D., Satish, M.G., El-Jabi, N., 2011. Study of stream temperature dynamics and corresponding heat fluxes within Miramichi River catchments (New Brunswick, Canada). *Hydrol. Process.* 25, 2439–2455. <https://doi.org/10.1002/hyp.8021>
- Heidbüchel, I., Troch, P.A., Lyon, S.W., Weiler, M., 2012. The master transit time distribution of variable flow systems. *Water Resour. Res.* 48. <https://doi.org/10.1029/2011WR011293>
- Hennig, C., 2007. Cluster-wise assessment of cluster stability. *Comput. Stat. Data Anal.* 52, 258–271. <https://doi.org/10.1016/j.csda.2006.11.025>
- Herb, W.R., Janke, B., Mohseni, O., Stefan, H.G., 2008. Thermal pollution of streams by runoff from paved surfaces. *Hydrol. Process.* 22, 987–999. <https://doi.org/10.1002/hyp.6986>
- Hester, E.T., Doyle, M.W., 2011. Human impacts to river temperature and their effects on biological processes: A quantitative synthesis. *J. Am. Water Resour. Assoc.* 47, 571–587. <https://doi.org/10.1111/j.1752-1688.2011.00525.x>
- Hood, E., Gooseff, M.N., Johnson, S.L., 2006. Changes in the character of stream water dissolved organic carbon during flushing in three small watersheds, Oregon. *J. Geophys. Res. Biogeosciences* 111. <https://doi.org/10.1029/2005JG000082>
- Inamdar, S., Singh, S., Dutta, S., Levia, D., Mitchell, M., Scott, D., Bais, H., McHale, P., 2011. Fluorescence characteristics and sources of dissolved organic matter for stream water during storm events in a forested mid-Atlantic watershed. *J. Geophys. Res. Biogeosciences* 116. <https://doi.org/10.1029/2011JG001735>
- Jencso, K.G., McGlynn, B.L., Gooseff, M.N., Wondzell, S.M., Bencala, K.E., Marshall, L.A., 2009. Hydrologic connectivity between landscapes and streams: Transferring reach- and plot-scale understanding to the catchment scale. *Water Resour. Res.* 45. <https://doi.org/10.1029/2008WR007225>
- Kaufman, L., Rousseeuw, P.J., 2009. *Finding Groups in Data: An Introduction to Cluster Analysis*. John Wiley & Sons.
- Kaufman, L., Rousseeuw, P.J., 1990. Clustering Large Applications, in: *Finding Groups in Data*. John Wiley & Sons, Ltd, pp. 126–163. <https://doi.org/10.1002/9780470316801.ch3>
- Keppeler, E.T., Brown, D., 1998. Subsurface drainage processes and management impacts, in: Ziemer, R.R. (Ed.), *Proceedings of the Conference on Coastal Watersheds: The Caspar Creek Story*, May 6, 1998, Ukiah, California. U.S. Forest Service Pacific Southwest Research Station, General Technical Report PSW GTR-168, Albany, CA, pp. 25–34.
- Kobayashi, D., Ishii, Y., Kodama, Y., 1999. Stream temperature, specific conductance and runoff process in mountain watersheds. *Hydrol. Process.* 13, 865–876. [https://doi.org/10.1002/\(SICI\)1099-1085\(19990430\)13:6<865::AID-HYP761>3.0.CO;2-O](https://doi.org/10.1002/(SICI)1099-1085(19990430)13:6<865::AID-HYP761>3.0.CO;2-O)

- Kuglerová, L., Ågren, A., Jansson, R., Laudon, H., 2014. Towards optimizing riparian buffer zones: Ecological and biogeochemical implications for forest management. *For. Ecol. Manag.* 334, 74–84. <https://doi.org/10.1016/j.foreco.2014.08.033>
- Lange, J., Haensler, A., 2012. Runoff generation following a prolonged dry period. *J. Hydrol.* 464–465, 157–164. <https://doi.org/10.1016/j.jhydrol.2012.07.010>
- Larsen, L.G., Woelfle-Erskine, C., 2018. Groundwater is key to salmonid persistence and recruitment in intermittent Mediterranean-climate streams. *Water Resour. Res.* 54, 8909–8930. <https://doi.org/10.1029/2018WR023324>
- Laudon, H., Kuglerová, L., Sponseller, R.A., Futter, M., Nordin, A., Bishop, K., Lundmark, T., Egnell, G., Ågren, A.M., 2016. The role of biogeochemical hotspots, landscape heterogeneity, and hydrological connectivity for minimizing forestry effects on water quality. *Ambio* 45, 152–162. <https://doi.org/10.1007/s13280-015-0751-8>
- Leach, J.A., Lidberg, W., Kuglerová, L., Peralta-Tapia, A., Ågren, A., Laudon, H., 2017. Evaluating topography-based predictions of shallow lateral groundwater discharge zones for a boreal lake-stream system. *Water Resour. Res.* 53, 5420–5437. <https://doi.org/10.1002/2016WR019804>
- Leach, J.A., Moore, D., 2017. Insights on stream temperature processes through development of a coupled hydrologic and stream temperature model for forested coastal headwater catchments. *Hydrol. Process.* 31, 3160–3177. <https://doi.org/10.1002/hyp.11190>
- Leach, J.A., Moore, R.D., 2015. Observations and modeling of hillslope throughflow temperatures in a coastal forested catchment. *Water Resour. Res.* 3770–3795. <https://doi.org/10.1002/2014WR016763>
- Leach, J.A., Moore, R.D., 2014. Winter stream temperature in the rain-on-snow zone of the Pacific Northwest: Influences of hillslope runoff and transient snow cover. *Hydrol. Earth Syst. Sci.* 18, 819–838. <https://doi.org/10.5194/hess-18-819-2014>
- Leach, J.A., Olson, D.H., Anderson, P.D., Eskelson, B.N.I., 2016. Spatial and seasonal variability of forested headwater stream temperatures in western Oregon, USA. *Aquat. Sci.* 79, 291–307. <https://doi.org/10.1007/s00027-016-0497-9>
- Liu, W., Birgand, F., Tian, S., Chen, C., 2021. Event-scale hysteresis metrics to reveal processes and mechanisms controlling constituent export from watersheds: A review☆. *Water Res.* 200, 117254. <https://doi.org/10.1016/j.watres.2021.117254>
- Lloyd, C.E.M., Freer, J.E., Johnes, P.J., Collins, A.L., 2016a. Using hysteresis analysis of high-resolution water quality monitoring data, including uncertainty, to infer controls on nutrient and sediment transfer in catchments. *Sci. Total Environ.* 543, 388–404. <https://doi.org/10.1016/j.scitotenv.2015.11.028>
- Lloyd, C.E.M., Freer, J.E., Johnes, P.J., Collins, A.L., 2016b. Technical Note: Testing an improved index for analysing storm discharge-concentration hysteresis. *Hydrol. Earth Syst. Sci.* 20, 625–632. <https://doi.org/10.5194/hess-20-625-2016>
- Loperfido, J. V., Just, C.L., Schnoor, J.L., 2009. High-frequency diel dissolved oxygen stream data modeled for variable temperature and scale. *J. Environ. Eng.* 135, 1250–1256. [https://doi.org/10.1061/\(ASCE\)EE.1943-7870.0000102](https://doi.org/10.1061/(ASCE)EE.1943-7870.0000102)
- Lowry, C.S., Walker, J.F., Hunt, R.J., Anderson, M.P., 2007. Identifying spatial variability of groundwater discharge in a wetland stream using a distributed temperature sensor. *Water Resour. Res.* 43, 1–9. <https://doi.org/10.1029/2007WR006145>
- MacDonald, R.J., Boon, S., Byrne, J.M., Robinson, M.D., Rasmussen, J.B., 2014. Potential future climate effects on mountain hydrology, stream temperature, and native salmonid

- life history. *Can. J. Fish. Aquat. Sci.* 71, 189–202. <https://doi.org/10.1139/cjfas-2013-0221>
- Mahoney, M., Magel, R., 1996. Estimation of the Power of the Kruskal-Wallis Test. *Biom. J.* 38, 613–630. <https://doi.org/10.1002/bimj.4710380510>
- Mistick, E., Johnson, M.S., 2020. High-frequency analysis of dissolved organic carbon storm responses in headwater streams of contrasting forest harvest history. *J. Hydrol.* 590, 125371. <https://doi.org/10.1016/j.jhydrol.2020.125371>
- Moore, R.D., Spittlehouse, D.L., Story, A., 2005. Riparian microclimate and stream temperature response to forest harvesting: A review. *J. Am. Water Resour. Assoc.* 41, 813–834. <https://doi.org/10.1111/j.1752-1688.2005.tb04465.x>
- Olden, J.D., Kennard, M.J., Pusey, B.J., 2012. A framework for hydrologic classification with a review of methodologies and applications in ecohydrology. *Ecohydrology* 5, 503–518. <https://doi.org/10.1002/eco.251>
- Oware, E.K., Peterson, E.W., 2020. Storm driven seasonal variation in the thermal response of the streambed water of a low-gradient stream. *Water Switz.* 12, 40–44. <https://doi.org/10.3390/w12092498>
- Ozaki, N., Fukushima, T., Harasawa, H., Kojiri, T., Kawashima, K., Ono, M., 2003. Statistical analyses on the effects of air temperature fluctuations on river water qualities. *Hydrol. Process.* 17, 2837–2853. <https://doi.org/10.1002/hyp.1437>
- Penna, D., van Meerveld, H.J., Oliviero, O., Zuecco, G., Assendelft, R.S., Dalla Fontana, G., Borga, M., 2015. Seasonal changes in runoff generation in a small forested mountain catchment. *Hydrol. Process.* 29, 2027–2042.
- Ploum, S.W., Leach, J.A., Kuglerová, L., Laudon, H., 2018. Thermal detection of discrete riparian inflow points (DRIPs) during contrasting hydrological events. *Hydrol. Process.* 32, 3049–3050. <https://doi.org/10.1002/hyp.13184>
- Poole, G.C., Risley, J., Hicks, M., 2001. Issue Paper 3 Spatial and Temporal Patterns of Stream Temperature (Revised). *Environ. Prot.*
- PRISM Climate Group, 2014. PRISM gridded climate data. Oregon State University. [WWW Document]. URL <https://prism.oregonstate.edu> (accessed 5.17.22).
- Radke, A.G., Godsey, S.E., Lohse, K.A., McCorkle, E.P., Perdrial, J., Seyfried, M.S., Holbrook, W.S., 2019. Spatiotemporal heterogeneity of water flowpaths controls dissolved organic carbon sourcing in a snow-dominated, headwater catchment. *Front. Ecol. Evol.* 7. <https://doi.org/10.3389/fevo.2019.00046>
- Rinderer, M., Van Meerveld, H.J., Seibert, J., 2014. Topographic controls on shallow groundwater levels in a steep, prealpine catchment. *Water Resour. Res.* 50, 6067–6080. <https://doi.org/10.1002/2013WR015009>
- Rousseeuw, P.J., 1987. Silhouettes: A graphical aid to the interpretation and validation of cluster analysis. *J. Comput. Appl. Math.* 20, 53–65. [https://doi.org/10.1016/0377-0427\(87\)90125-7](https://doi.org/10.1016/0377-0427(87)90125-7)
- Schlosser, I.J., 1991. Stream Fish Ecology : A Landscape Perspective 41, 704–712.
- Segura, C., Noone, D., Warren, D., Jones, J.A., Tenny, J., Ganio, L.M., 2019. Climate, Landforms, and Geology Affect Baseflow Sources in a Mountain Catchment. *Water Resour. Res.* 55, 5238–5254. <https://doi.org/10.1029/2018WR023551>
- Shanley, J.B., Peters, N.E., 1988. Preliminary observations of streamflow generation during storms in a forested Piedmont watershed using temperature as a tracer. *J. Contam. Hydrol.* 3, 349–365. [https://doi.org/10.1016/0169-7722\(88\)90040-X](https://doi.org/10.1016/0169-7722(88)90040-X)

- Sharghi, E., Nourani, V., Soleimani, S., Sadikoglu, F., 2018. Application of different clustering approaches to hydroclimatological catchment regionalization in mountainous regions, a case study in Utah State. *J. Mt. Sci.* 15, 461–484. <https://doi.org/10.1007/s11629-017-4454-4>
- Sidle, R.C., Tsuboyama, Y., Noguchi, S., Hosoda, I., Fujieda, M., Shimizu, T., 2000. Stormflow generation in steep forested headwaters: A linked hydrogeomorphic paradigm. *Hydrol. Process.* 14, 369–385. [https://doi.org/10.1002/\(SICI\)1099-1085\(20000228\)14:3<369::AID-HYP943>3.0.CO;2-P](https://doi.org/10.1002/(SICI)1099-1085(20000228)14:3<369::AID-HYP943>3.0.CO;2-P)
- Siegel, S., 1957. Nonparametric Statistics. *Am. Stat.* 11, 13–19. <https://doi.org/10.1080/00031305.1957.10501091>
- Sklash, M.G., Farvolden, R.N., 1979. The role of groundwater in storm runoff. *J. Hydrol.* 43, 45–65. [https://doi.org/10.1016/0022-1694\(79\)90164-1](https://doi.org/10.1016/0022-1694(79)90164-1)
- Snedecor, G.W., 1956. *Statistical methods: applied to experiments in agriculture and biology.* The Iowa state college press.
- Snyder, C.D., Hitt, N.P., Young, J.A., 2015. Accounting for groundwater in stream fish thermal habitat responses to climate change. *Ecol. Appl.* 25, 1397–1419. <https://doi.org/10.5061/dryad.th6g8>
- Soil Survey Staff, NRCS, U., 2016. Coppercreek and Sasquatch Series: Official Soil Series Descriptions.
- Somers, K.A., Bernhardt, E.S., Mcglynn, B.L., Urban, D.L., 2016. Downstream Dissipation of Storm Flow Heat Pulses: A Case Study and its Landscape-Level Implications. *J. Am. Water Resour. Assoc.* 52, 281–297. <https://doi.org/10.1111/1752-1688.12382>
- Subehi, L., Fukushima, T., Onda, Y., Mizugaki, S., Gomi, T., Kosugi, K., Hiramatsu, S., Kitahara, H., Kuraji, K., Terajima, T., 2010. Analysis of stream water temperature changes during rainfall events in forested watersheds. *Limnology* 11, 115–124. <https://doi.org/10.1007/s10201-009-0296-2>
- Surfleet, C., Louen, J., 2018. The influence of hyporheic exchange on water temperatures in a headwater stream. *Water Switz.* 10. <https://doi.org/10.3390/w10111615>
- Tiwari, T., Lundström, J., Kuglerová, L., Laudon, H., Öhman, K., Ågren, A.M., 2016. Cost of riparian buffer zones: A comparison of hydrologically adapted site-specific riparian buffers with traditional fixed widths. *Water Resour. Res.* <https://doi.org/10.1002/2015WR018014>
- Tongal, H., Sivakumar, B., 2017. Cross-entropy clustering framework for catchment classification. *J. Hydrol.* 552, 433–446. <https://doi.org/10.1016/j.jhydrol.2017.07.005>
- Uchida, T., Kosugi, K., Mizuyama, T., 2002. Effects of pipe flow and bedrock groundwater on runoff generation in a steep headwater catchment in Ashiu, Central Japan. *Water Resour. Res.* 38, 24-1-24–14. <https://doi.org/10.1029/2001wr000261>
- Van Meerveld, H J, Seibert, J., Peters, N.E., 2015. Hillslope-riparian-stream connectivity and flow directions at the Panola Mountain Research Watershed. *Hydrol. Process.* 29, 3556–3574. <https://doi.org/10.1002/hyp.10508>
- Van Meerveld, H. J., Seibert, J., Peters, N.E., 2015. Hillslope–riparian-stream connectivity and flow directions at the Panola Mountain Research Watershed. *Hydrol. Process.* 29, 3556–3574.
- Vaughan, M.C.H., Bowden, W.B., Shanley, J.B., Vermilyea, A., Sleeper, R., Gold, A.J., Pradhanang, S.M., Inamdar, S.P., Levia, D.F., Andres, A.S., Birgand, F., Schroth, A.W., 2017. High-frequency dissolved organic carbon and nitrate measurements reveal

- differences in storm hysteresis and loading in relation to land cover and seasonality. *Water Resour. Res.* <https://doi.org/10.1002/2017WR020491>
- Wang, L., Liu, H., 2006. An efficient method for identifying and filling surface depressions in digital elevation models for hydrologic analysis and modelling. *Int. J. Geogr. Inf. Sci.* 20, 193–213. <https://doi.org/10.1080/13658810500433453>
- Webb, B.W., Hannah, D.M., Moore, R.D., Brown, L.E., Nobilis, F., 2008. Recent advances in stream and river temperature research. *Hydrol. Process.* 22, 902–918. <https://doi.org/10.1002/hyp.6994>
- Webb, B.W., Zhang, Y., 1997. Spatial and seasonal variability in the components of the river heat budget. *Hydrol. Process.* 11, 79–101. [https://doi.org/10.1002/\(SICI\)1099-1085\(199701\)11:1<79::AID-HYP404>3.0.CO;2-N](https://doi.org/10.1002/(SICI)1099-1085(199701)11:1<79::AID-HYP404>3.0.CO;2-N)
- Wilby, R.L., Johnson, M.F., Toone, J.A., 2015. Thermal shockwaves in an upland river. *Weather* 70, 92–100. <https://doi.org/10.1002/wea.2435>
- Wilby, R.L., Johnson, M.F., Toone, J.A., 2014. Nocturnal river water temperatures: Spatial and temporal variations. *Sci. Total Environ.* 482–483, 157–173. <https://doi.org/10.1016/j.scitotenv.2014.02.123>
- Williams, G.P., 1989. Sediment concentration versus water discharge during single hydrologic events in rivers. *J. Hydrol.* 111, 89–106. [https://doi.org/10.1016/0022-1694\(89\)90254-0](https://doi.org/10.1016/0022-1694(89)90254-0)
- Wondzell, S.M., Gooseff, M.N., 2013. Geomorphic Controls on Hyporheic Exchange Across Scales: Watersheds to Particles, in: Shroder, J., Wohl, E. (Eds.), *Treatise on Geomorphology*. Academic Press, San Diego, CA, pp. 203–218. <https://doi.org/10.1016/B978-0-12-374739-6.00238-4>
- Woodward, J.S., Lamphear, D.W., House, M.R., 2011. General Technical Report PSW-GTR-238: Delineation of Preventative Landslide Buffers Along Steep Streamside Slopes in Northern California.
- Wu, H.Q., Huang, Q., Xu, W., Xi, S.F., 2015. Application of K-Means Cluster and Rough Set in Classified Real-Time Flood Forecasting. *Adv. Mater. Res.* 1092–1093, 734–741. <https://doi.org/10.4028/www.scientific.net/AMR.1092-1093.734>
- Zimmer, M.A., McGlynn, B.L., 2018. Lateral, Vertical, and Longitudinal Source Area Connectivity Drive Runoff and Carbon Export Across Watershed Scales. *Water Resour. Res.* 54, 1576–1598. <https://doi.org/10.1002/2017WR021718>
- Zimmer, M.A., McGlynn, B.L., 2017. Ephemeral and intermittent runoff generation processes in a low relief, highly weathered catchment. *Water Resour. Res.* 53, 7055–7077. <https://doi.org/10.1002/2016WR019742>